Flame Stabilization and Mixing Studies in a Novel Ultra-Low Emissions Combustor

M. K. Bobba,[*] P. Gopalakrishnan,[*] A. Radhakrishnan,[*] J. M. Seitzman,[†]
Y. Neumeier,[‡] B. T. Zinn[§] and J. Jagoda[**]

School of Aerospace Engineering,
Georgia Institute of Technology,
Atlanta, GA, USA,

The operation of a Stagnation Point Reverse Flow (SPRF) combustor is studied over a range of equivalence ratios and loadings. Previous studies have shown this combustor geometry can operate stably, even at low equivalence ratios, without the need of external preheating or swirl, while producing low pollutant emissions levels in both premixed and non-premixed modes. The SPRF combustion and mixing characteristics are investigated with a variety of imaging diagnostics: simultaneous OH PLIF and chemiluminescence (heat release) measurements, and laser scattering of oil droplets seeded into the fuel. Results indicate that the flame is primarily stabilized and that most of the heat release occurs in the downstream portion of the combustor, where there is a low mean velocity but high fluctuations. The hot products created in this region reverse direction and are entrained into the oncoming reactants. This increases chemical rates and flame speeds, contributing to the stability of the combustor. Fuel and air injected separately in case of non-premixed operation, are found to be mostly mixed by the time they reach the flame zone, allowing this combustor to operate with nearly the pollutant emissions levels of a premixed combustor, but without the safety concerns associated with premixing.

I. Introduction

Stringent emissions regulations on gas turbine engines have forced gas turbine manufacturers towards combustor designs that rely on lean premixed or partially premixed combustion. Ensuring that combustion occurs at locally lean conditions reduces peak flame temperatures and hence lowers NOx emission levels. At the same time, however, leaner mixtures result in weaker combustion, which makes the combustor less stable. Flame stability is improved by preheating the incoming reactants and by recirculation of hot exhaust gases. Gupta[1, 2] reported that flames with highly preheated combustion air were much more stable and homogeneous (both temporally and spatially) as compared to room-temperature combustion air and hence could operate at much leaner equivalence ratios. However, preheating raises flame temperatures, so that NOx reductions achieved by lowering the fuel-air ratio can be offset by increased NOx due to preheating. In most premixed combustors employed in land-based gas turbines, stabilization is partially achieved by swirl-induced internal recirculation of products and reactants.[3] Very high levels of internal recirculation in combustors, combined with other restrictions such as significant combustor heat loss, can lead to "flameless oxidation," where no visually distinct flame is observed.[4, 5]

---

[*] Graduate Research Assistant (AIAA student member)
[†] Associate Professor (AIAA Associate Fellow)
[‡] Adjunct Professor (AIAA Member)
[§] Davis S. Lewis Jr. Chair and Regents' Professor (AIAA Fellow)
[**] Professor (AIAA Associate Fellow)

Another difficulty in the operation of premixed systems is flame flashback and autoignition. High temperatures in a premixer can result in damage or shutdown of an engine. Hence, it is advantageous if fuel and air can be injected into the combustor separately and then allowed to mix rapidly before they burn. A new, compact combustor design that incorporates some of these approaches has recently been demonstrated.[6] The combustor design is open at one and closed at the other. As seen in the flow schematic of the combustor in Figure 1a, the reactants injected into the combustor along the centerline from the open end slow down as they reach the closed end and the product gases move back and leave the combustor through the open end, adjacent to the incoming reactants. Thus, the new design has been designated the Stagnation-Point Reverse-Flow (SPRF) combustor. The SPRF design is characterized by a rapidly decaying reactant jet with high turbulence levels (based on PIV measurements[7] at an equivalence ratio of $\phi = 0.58$ and loading of 8.1 g/s). The flow is also characterized by high turbulence intensities (varying from ~25-90% along the centerline between 1/3 and 2/3 of the combustor length). Such high turbulence can promote significant mixing of fuel, air and hot products. The combustor also exhibits good stability, even at quite lean equivalence ratios and high loadings.[6]

To better elucidate how mixing and stabilization are enhanced in the SPRF combustor geometry, this paper reports measurements in an atmospheric-pressure, SPRF combustor operating in premixed and nonpremixed modes, i.e., with reactants either well-mixed before entering the combustor or with fuel and air entering the combustor separately. Planar Laser Induced Fluorescence (PLIF)[8] of the OH radical is used to visualize the combustion zone and hot product gases. Dark region with no OH signal indicates regions of unburnt fuel-air. Therefore, OH PLIF can also provide some information on the mixing of hot products and cold reactants. This technique has been successfully used to study similar turbulent jet flames.[9] The OH PLIF measurements are also complemented by simultaneous imaging measurements of chemiluminescence from CH^* and CO_2^*, which mark zones of heat release. Finally, laser light scattered from droplets seeded into the fuel stream provides information on mixing of fuel with air and hot products when the combustor operates nonpremixed.

II. Experimental Setup

The atmospheric pressure embodiment of the SPRF combustor employed in this study is shown in Figure 1. It consists of a quartz tube (303 mm long and 70 mm in diameter), with a quartz disc inserted into the bottom to close one end of the tube (Figure 1a). Quartz has been used for the combustor wall as it can sustain high temperatures while allow optical access for the diagnostics techniques mentioned above. The laser sheet enters the combustor through the base plate and emitted light is collected perpendicular to it. To reduce heat losses, the combustor can also be insulated by surrounding the quartz tube with a cylinder of alumina (ZIRCAR AL-30AAH). The insulation is further cut into four smaller cylinders, with a window cut out of one of them. These rings (shown in Figure 1b), can be stacked as required to be able view any part of the combustor. The injector in this combustor consists of a co-annular tube configuration (without swirl), with an outer diameter of 12.5 mm. In the premixed mode of operation, both fuel (natural gas) and air are injected through the outer annulus while the inner tube is closed off upstream. In the nonpremixed case, fuel comes in through the inner tube with a co-flow of air injected through the outer annulus. This injection configuration allows for easy switching of the combustor between premixed and nonpremixed modes. Fuel and air flow rates into the combustor are monitored independently and controlled to produce a range of equivalence ratios and flow velocities.

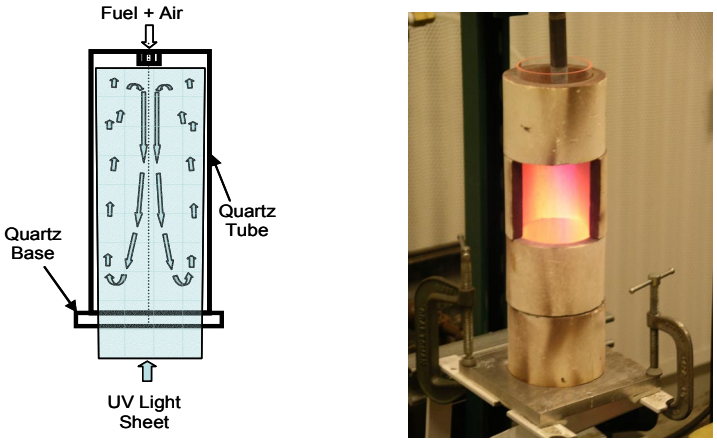

Figure 1. Schematic and photographic of the operating SPRF combustor.

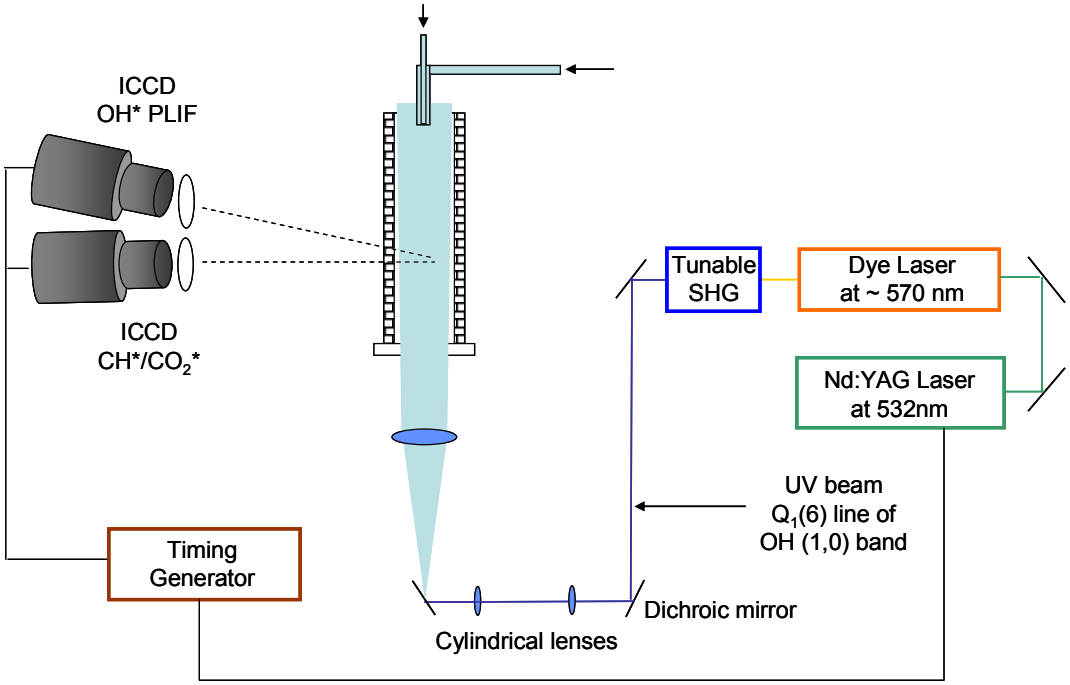

Figure 2. Experimental layout employed for the optical diagnostics.

The OH PLIF system, as shown in the optical layout of Figure 2, consists a Lambda Physik dye laser system pumped by the second harmonic of a Nd:YAG laser. The output from this dye laser system (around 570 nm) is frequency-doubled using a tunable second harmonic generator (Inrad Autotracker, BBO crystal). The portion of light whose frequency is successfully doubled is separated from the rest of the light with a set of three dichroic turning mirrors. The resulting ultraviolet (UV) laser beam is then expanded into a sheet that is 65 mm wide and 300 μm thick with three fused silica lenses. The UV sheet enters the combustor through the quartz disk at the bottom and illuminates the complete length, and nearly the complete width of the combustor. The wavelength of the dye laser beam is calibrated by measuring an OH excitation scan in a reference flame and comparing it to a standard (predicted) OH spectrum for the $A^2\Sigma^+(v'=1)\leftarrow X^2\Pi(v''=0)$ band. The laser is then tuned to the $Q_1(6)$ line of the (1,0) band. The average energy of the laser pulses (~10 ns long) entering the combustor was measured to be 12 mJ, and the shot-to-shot variation in pulse energy during the experiments was less than 15%. The emitted fluorescence light is detected at right angles to the laser sheet using a 25 mm intensified PI-MAX camera equipped (256×1024 pixels) with a UV-Nikkor lens system (105 mm, f#4). The detected fluorescence signal is limited to 300–370 nm by WG305 and UG 11Schott glass filters placed in front of the camera lens. The camera's field of

view includes the whole width of the combustor in all the images, which results in a pixel resolution of approximately 300 µm.

The flame chemiluminescence emitted by chemically produced CH^* and CO_2^* molecules in the flame zone is also imaged at right angles to the laser sheet. The light is collected with a separate intensified camera (Princeton Instruments ICCD-576-S/RB-E with 18mm intensifier and 384×576 pixels) equipped with a narrow band interference filter that passes CH emission around 430 nm, along with a fraction of the broadband CO_2^* signal in that wavelength range. The camera is synchronized such that the exposure (250 µs long) begins 100 ns after the OH laser pulse. This allows for complete decay of the OH fluorescence before the chemiluminescence image is recorded. Thus both cameras record nearly simultaneous features of the combustor. The field of view for this camera is also set to see the whole width of the combustor with a pixel resolution of 250 µm. Images of a reference grid are recorded with both cameras, and these are used to spatially match the corresponding PLIF and chemiluminescence frames.

Laser scattering from olive oil droplets (average diameter of 5-10 µm) injected into the fuel stream is imaged with a standard particle image velocimetry (PIV) setup used in a companion effort.[7] A change (reduction) in scattered intensity from the droplets can occur due to dilution as the droplets mix with surrounding air or due to evaporation of the droplets as they are heated as they approach a flame zone or are mixed with hot products gases. Based on a standard evaporation model for liquid droplets, it is predicted that olive oil droplets (570K boiling point) with a diameter of 7 µm and with velocities above 50 m/s (a lower value than the velocities expected in the region near the fuel injector) would experience a rapid drop in scattering intensity due to evaporation for temperatures above ~900-1100 K. Hence, it may be inferred that the regions where droplets are observed in these experiments represent locations where the local temperature does not exceed ~900-1100 K.

III. Results and Discussion

The influence of the flowfield features described in the background, on flame anchoring mechanisms was first investigated by imaging the OH field for *stoichiometric* mixtures over a range of combustor loadings. The insulation was removed in order to image the full combustor flowfield at one time. Figure 3 shows instantaneous PLIF frames at different combustor loadings, i.e., different reactant mass flowrates. To emphasize flame stabilization processes, these images display only the region near the injector (and thus also the exit). In OH PLIF images, a reaction zone is usually indicated by a sharp gradient in the PLIF signal adjacent to reactant gases. For the lowest loading (0.14 g/s), the flow is nearly laminar (Re~500), and the flame is an annular Bunsen flame, the cross section of which can be seen in Figure 3a. The flame is stabilized in two locations. The outer portion of the flame is stabilized on the outer rim of the injector, while the inner portion is stabilized in the bluffbody-like recirculation zone that is formed because the inner tube of the annular injector is closed upstream in premixed operation. At this low velocity condition (Figure 3a), the flame sits very close to the injector. The OH concentration peaks just downstream of the reaction zone and decreases as the product gases cool off. This is due to the high sensitivity of equilibrium OH

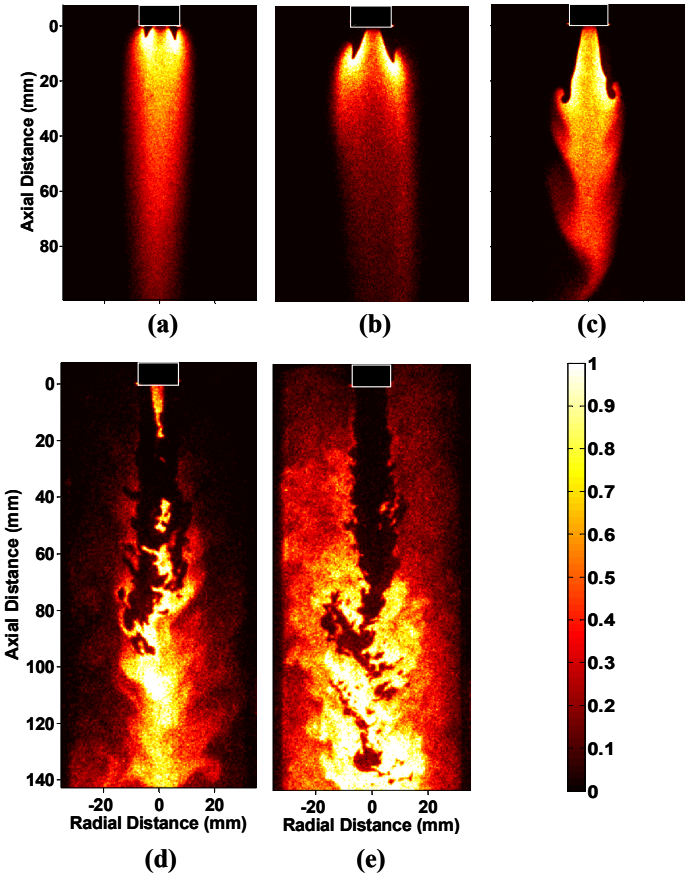

Figure 3. Single shot PLIF images showing near-injector region in the combustor at $\phi = 1$ and loadings of (a) 0.14 (b) 0.2 (c) 0.43 (d) 1.8 and (e) 5.7 g/s.

concentration to temperature. For increasing injection velocity (Figure 3b,c), the increased strain in the flow causes the flame to progressively lift from the outer rim, while it still remains anchored on the inner recirculation zone. For these low flowrate conditions (below ~0.5 g/s), the shear between the inflow and exhaust is low. Also, the reverse flowing products are cooled by heat losses to the combustor walls. This can be seen from the lack of OH PLIF signal in the exhaust gases.

At higher flowrates, the entrainment of *high temperature* products (marked by the presence of OH in the products) becomes strong enough to stabilize a flame again on the outer rim (Figure 3d,e). Since the velocity of the reverse flowing products increases as the entering reactant flowrate is raised, the entrainment of products into the reactant stream is likely enhanced by the increased shear between the two flows at these conditions. For the 1.8 g/s loading (Figure 3d), a small reaction zone in seen in the inner recirculation region, but it is not able to stabilize a flame in the high velocity reactants. There appears to be a flame in the shear/mixing layer between the reactants and products. At higher loadings (Figure 3e), the inner recirculation reaction zone disappears, and the flame in the outer shear layer extends nearly back to the injector.

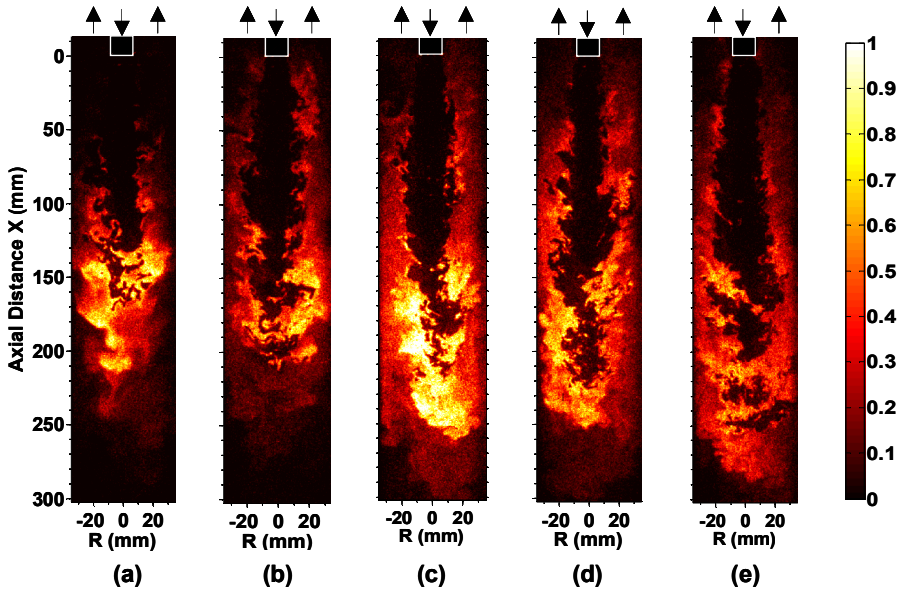

Figure 4. Instantaneous PLIF images covering the whole combustor at ϕ = 0.65 at loadings of (a) 2 (b) 4.5 (c) 7.2 (d) 9.4 and (e) 10.7 g/s. Reynolds number based on injector diameter is estimated to vary from 10,000 to 57,000 for lowest to the highest loading case.

The effect of variation of loading on the penetration of reactants into this stabilization region mentioned above is investigated at a leaner equivalence ratio, ϕ=0.65 (see Figure 4). The combustor configuration is similar to the one used in the previous set of experiments and the camera's field of view has been adjusted to image the complete length of the combustor. The dark region extending from the injector in the instantaneous OH PLIF images represent the reactants entering the combustor. The reactant jet is found to penetrate somewhat deeper into the combustor with higher injection velocities (Figures 4a-e). The stagnation condition imposed by the end wall, however, makes the jet penetration much less sensitive to loading at high loading conditions (e.g., Figures 4c-e) than conventional combustors, where flame length continues to increase with loading. The high OH concentrations at the bottom of the combustor (x = 120-230 mm) suggests that the temperatures there are high or that much of the heat release occurs in this region. This roughly coincides with the low average velocity region observed in the velocity data[7] for the insulated combustor operating lean and at high loadings. This suggests that the flame in the combustor is also stabilized by a possible second stabilization mechanism. High turbulence intensity in this part of the combustor creates a highly distorted flame front (seen in Figure 4) that can propagate against a relatively low mean flow. Like the stabilization process near the outer rim of the injector discussed earlier, any entrainment of hot products into the reactants before reaching the low velocity region will also tend to

increase the flame speed and lowering ignition energies as suggested by Kalb and Sattelmayer[10] and contribute to the stability of the combustor.

The entrainment of hot products and radicals back into the reactants aids the stabilization of the flame. Therefore reducing the amount of heat loss by insulating the combustor should make the flame more stable, allowing the combustor to operate stably at leaner equivalence ratios and high loadings. Therefore, the insulation described previously was added around the quartz liner. Due to the presence of the insulation, PLIF and chemiluminescence images are acquired from a smaller region accessed through a window cut out of the insulation. The location of the imaging window can be moved, allowing imaging of any quarter of the combustor's length.

Figure 5 shows simultaneously acquired instantaneous PLIF and chemiluminescence images at a lean and high loading condition. Images acquired in windows at different times are stacked to see prominent features. The bottom portion of the combustor (x=230-303 mm) lacks interesting features, as seen in Figure 4. Hence images were not acquired from the bottom quarter of the combustor, and that region is represented by a blank frame in Figure 5. The region closest to the injector shows significant OH signal present in the product stream heading back, and the simultaneous chemiluminescence signal indicates the presence of a weak flame extending close to the injector. Reduced heat losses due to the insulation keeps the product gases hot and explains the higher OH levels seen in the product stream compared to the frames taken without the insulation (Figures 4a-e). Higher temperatures in the combustor due to the insulation and possibly more OH radicals entrainment into the reactant stream results in an increase in signal intensity in these reactant regions seen clearly in the PLIF image (Figure 5a) from x=145-230 mm Although the OH PLIF signal gradients are reduced due to product entrainment, the dark regions seen in these frames appear to fit just inside of the simultaneously measured chemiluminescence emission (Figure 5b), which is an indication of where heat release is occurring. This suggests a distinct flame-like structure, i.e., the reactants are probably not burning in a widely distributed reaction zone.

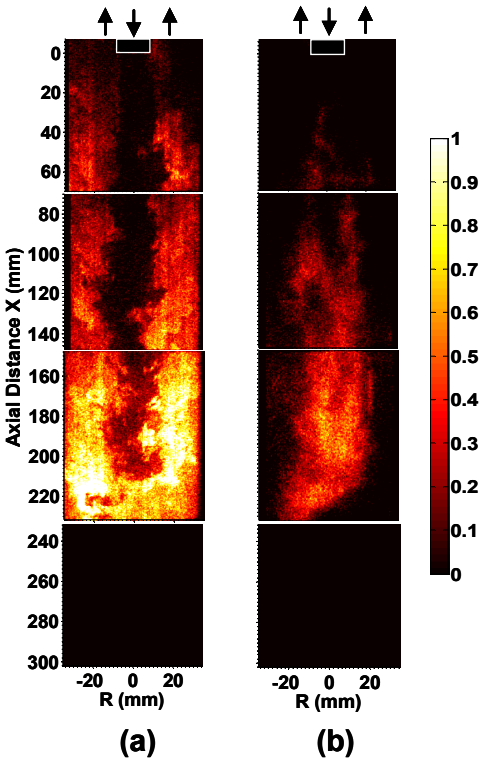

Figure 5. (a)Instantaneous OH and (b) simultaneous chemiluminescence images at ϕ =0.58 and a loading of 13.2 g/s in the premixed insulated combustor. Images of different axial locations acquired nonsimultaneously.

The presence of most of the chemiluminescence intensity in the highly turbulent, low velocity region referred to previously (x=120-230 mm) confirms the interpretation from the OH data regarding the stabilization zone. This interesting region is further explored by examining a set of correlated OH and chemiluminescence frames shown in Figure 6 acquired at the same flow conditions as the Figure 5 results. The chemiluminescence in these images again occurs around the dark reactant regions in the PLIF image but at high loadings, the reactant jet is found to become more unsteady. This unsteadiness in the flame zone can be clearly seen from the large movement of the heat release zone again suggesting the presence of large vortical structures in this region. The chemiluminescence signal is spatially integrated normal to the laser sheet and hence also captures out of plane heat release. This accounts for the small regions of heat release seen in a few of the chemiluminescence frames without a corresponding reactant region in the PLIF images marked in Figure 6. Having investigated the premixed mode of combustor operation in detail, the rest of the paper focuses on characterizing the non-premixed mode, which has been shown to produce similar pollutant emission levels as in premixed operation.[6]

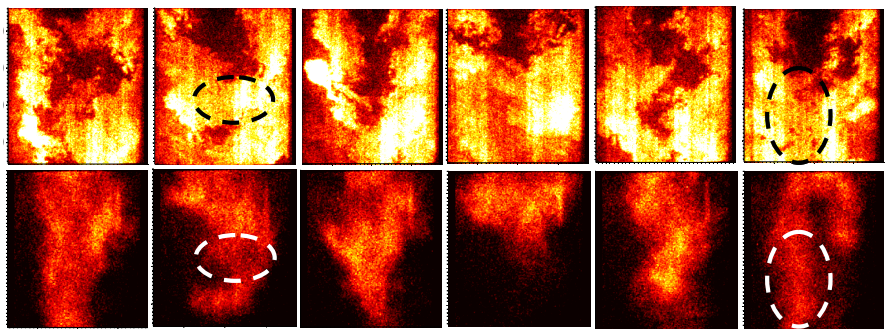

Figure 6. Set of single shot OH (top) and simultaneous chemiluminescence (bottom) image pairs acquired for a region of x=145-230 mm (ϕ = 0.58, loading of 13.2 g/s).

Figure 7 shows single shot PLIF images of both the premixed and nonpremixed combustor at two different equivalence ratios (ϕ = 0.65 and 0.8) and a fixed loading (7.2 g/s). These images were acquired without insulation to facilitate viewing of the complete combustor. A comparison of the PLIF frames between the premixed and non-premixed configurations of the combustor at the leaner equivalence ratio (Figures 7a and c respectively) indicate similar reactant penetration and structure except in the near field. The increase in equivalence ratio from 0.65 to 0.8 in the premixed mode at fixed loading (Figures 7a and b) produces a significantly shorter flame due to higher flame temperatures and hence higher reaction rates at higher equivalence ratios. This can also be seen as increased OH signals in the ϕ = 0.8 case. A similar variation of equivalence ratio in the non-premixed mode shows some interesting features (Figures 7c and d). Unlike mixing-limited, nonpremixed jet flames where flame length increases with an increase in fuel flowrate at a fixed air flowrate,[11] the flame regions indicated by the OH images tend to become shorter just like in the premixed case. This suggests a significant level of mixing of fuel with air (and product gases) before combustion occurs. Hence combustion in the non-premixed mode in this combustor is probably premixed or partially premixed and is not limited by fuel-air mixing. This also explains the similarity in the structure of the PLIF images between premixed and non-premixed modes.

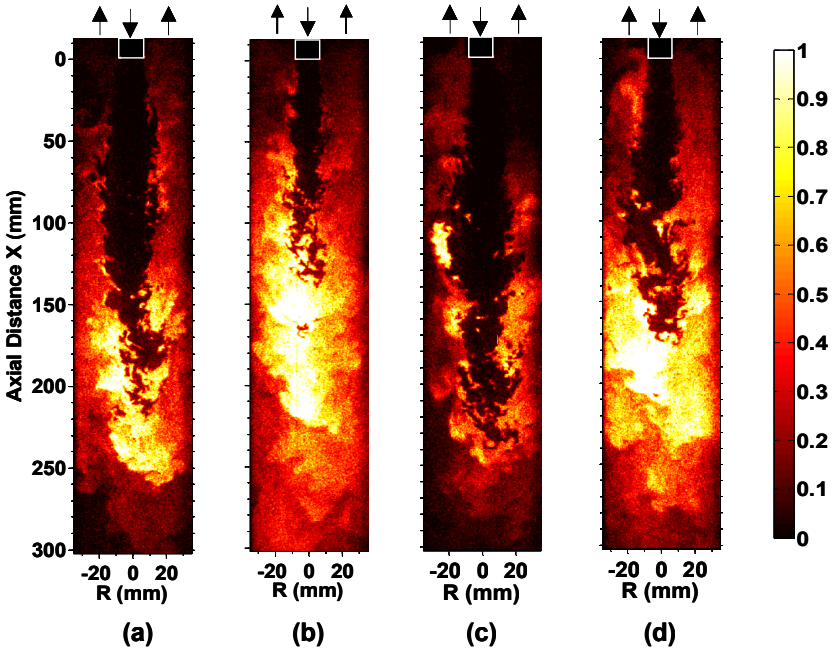

Figure 7. Single shot OH PLIF images in uninsulated combustor at loading of 7.2 g/s, comparing premixed and non-premixed mode of operation:(a) premixed mode (ϕ = 0.65) (b) premixed mode (ϕ = 0.8) (c) non-premixed mode (ϕ = 0.65) (d) non-premixed mode (ϕ = 0.8).

To compare the regions of heat release in both these modes, chemiluminescence images were recorded along with the OH PLIF. Figure 8 shows a comparison of the instantaneous chemiluminescence fields measured in the insulated combustor at a loading of 13.2 g/s and ϕ = 0.58. Images acquired in windows are again stacked to show the full combustor. The chemiluminescence image for the non-premixed mode of operation (Figure 8a), shows that most of the heat release in this case occurs for x= 140-230 mm. Unlike the premixed combustor (Figure 8b), there is negligible heat release close to the injector and the flame is completely lifted. This large standoff distance provides ample time for fuel and air to mix, and also to entrain product gases before reaching the flame zone.

This aspect of fuel and air mixing is further investigated by imaging light scattered from oil droplets seeded into the fuel. Figure 9 shows the variation of the normalized average, centerline droplet intensity with axial distance from the injector exit. Also shown is the average chemiluminescence intensity along the centerline obtained from averaging 300 frames of chemiluminescence images in the insulated combustor. The decrease in droplet scattering intensity is less than 20% within the first 40 mm. The corresponding chemiluminescence intensities in this region are negligible. These observations suggest some fuel-air mixing occurs here in this region, but little entrainment of products into the fuel stream. In other words, the fuel is initially shielded from the hot products by the annular air stream. Further downstream, the scattered intensities drop nearly linearly, until x~125 mm, at which point the droplet scattering is reduced to the local background level. The slow, nearly linear decrease in droplet scattering before this points suggests significant dilution of the fuel with air, and possibly some products but that the fraction of products is sufficiently low that temperatures under likely below 900-1100 K before x~125 mm. The rapid increase in average chemiluminescence (or heat release) for the region beyond x~125 mm, indicates temperatures beyond this region are high enough to rapidly evaporate the oil droplets.

Fuel entering the combustor is shielded from hot product gases by the co-flowing air stream. These data confirm that fuel and air mix rapidly in the initial region but it is still relatively cold. A flame can be sustained in the high velocities and strained zones only after this fuel-air mixture has entrained enough hot products. This shows that this combustor is not limited by fuel and air mixing but by mixing of fuel and air with hot products.

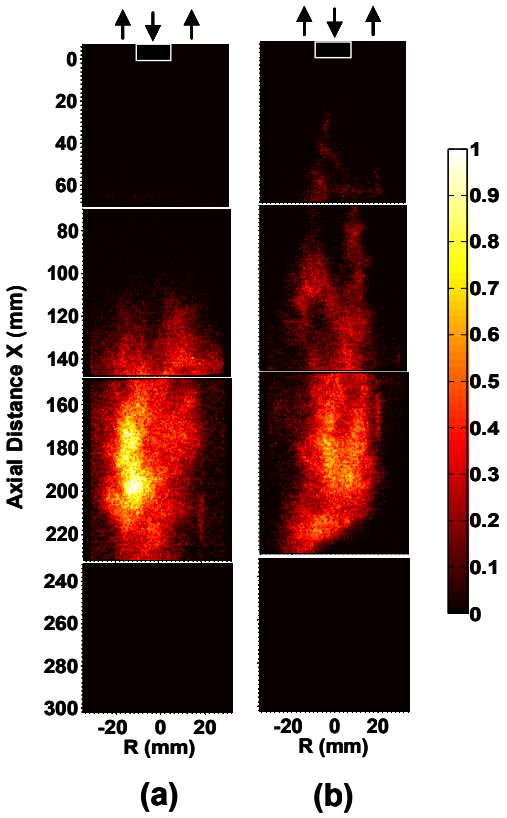

Figure 8. Comparison of instantaneous chemiluminescence images between (a) non-premixed mode (b) premixed mode at a loading of 13.2 g/s and ϕ = 0.58.

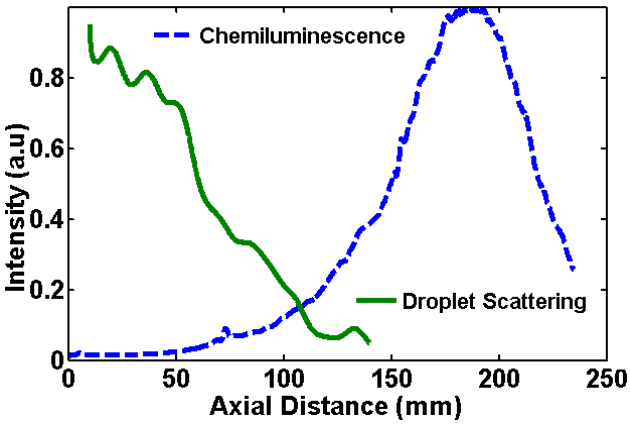

Figure 9. Variation of average chemiluminescence and average centerline droplet scattering intensities with the axial distance from the injector.

IV. Conclusions

Flame stabilization and mixing characteristics in a stagnation-point reverse-flow combustor have been investigated. The specific embodiment of the SPRF geometry studied here consists of a cylindrical combustor, with the reactant injector located at the axial center of the single open end of the cylinder. Various optical diagnostics were employed, including simultaneous measurements of OH concentration with PLIF and chemiluminescence emissions from CH^* and CO_2^*, and separate laser scattering images of oil droplets seeded into the gaseous fuel.

The results show that the combustion for both premixed and nonpremixed reactant injection is primarily stabilized in the bottom half of the combustor, where most of the heat release occurs. This region is characterized by low average velocities but intense turbulent fluctuations. In the case of premixed operation, another stabilization zone may exist in the shear/mixing layer at the outer rim of the injector, where hot products in the reverse exhaust flow can mix with incoming reactants. Both the OH and chemiluminescence data, however, indicate the flame there is weak. In the nonpremixed case, this initial shear layer flame does not exist, as the products in the exhaust can only mix with air that surrounds the incoming fuel. Simultaneous images of chemiluminescence, which show regions of heat release, and the OH images, which can be used to delineate unburned, low temperature reactants, indicate that burning occurs around distinct packets of reactants. Hence, the combustion appears to occur in a thin flame-like structure, as opposed to a broad distributed reaction zone. Fuel and air injected separately in the non-premixed mode are found to mix somewhat rapidly after entering the combustor, before significant mixing with hot products has occurred. However, reactant and product mixing is likely to occur before the reactants burn in the latter portion of the combustor. Thus it can be concluded that even in the case of non-premixed reactant injection, the flame burns in a premixed or mostly premixed mode, which explains why a previous study found comparable NOx emissions for premixed and nonpremixed operation of the SPRF combustor. This internal fuel-air and then fuel-air-product mixing allows the SPRF combustor to attain nearly premixed performance without the safety concerns associated with premixing.

Acknowledgments

This research was supported by NASA through the University Research, Engineering, and Technology Institute for Aeropropulsion and Power, under Grant/Cooperative Agreement Number NCC3-982.

References

[1]Gupta, A.K. Bolz, S. and Hasegawa, T, "Effect of Air Preheat and Oxygen Concentration on Flame Structure and Emission," Proc. ASME J. Energy Resources and Technology, Vol. 121, September, 1999, pp. 209-216.

[2]Gupta, A. K., "Flame Characteristics with High Temperature Air Combustion," AIAA-2000-0593, 38th Aerospace Sciences Meeting & Exhibit, January 2000, Reno NV.

[3]Lefebvre, A., "Gas Turbine Combustion," McGraw-Hill, 1983.

[4]Wunning, J.G. (2000), "Flameless Combustion in Thermal Process Technology," Second International Seminar on High Temperature Combustion, Stockholm, Sweden.

[5]Plessing T., Peters N., Wünning J.G., "Laser Optical Investigation of Highly Preheated Combustion with Strong Exhaust Gas Recirculation," Twenty – Seventh Symposium (International) on Combustion / The Combustion Institute, 1998, pp. 3197-3204.

[6]Neumeier, Y., Weksler, Y., Zinn, B. T., Seitzman, J. M., Jagoda, J. and Kenny, J., "Ultra Low Emissions Combustor with Non-Premixed Reactants Injection," AIAA 2005-3775 41st AIAA/ASME/SAE/ASEE Joint Propulsion Conference & Exhibit 10 - 13 July 2005, Tucson, Arizona.

[7]Gopalakrishnan, P., Undapalli, S., Bobba, M., Sankaran, V., Menon, S., Zinn, B. T., and Seitzman, J., "Measurements and modeling of the flowfield in an ultra-low emissions combustor," AIAA-2006-962 44th AIAA Aerospace Sciences Meeting and Exhibit, Reno, Nevada. Jan 9-12 2006.

[8]Seitzman, J. M. and Hanson, R. K., "Planar fluorescence imaging in gases," Instrumentation for Flows with Combustion, ed., A. M. K. P. Taylor, 1993.

[9]P. Griebel, R. Bombach, A. Inauen, R. Schären, S.,Schenker, P. Siewert, "Flame Characteristics And Turbulent Flame Speeds Of Turbulent, High-Pressure," Lean Premixed Methane/Air Flames, GT2005-68565, Proceedings of GT2005 ASME Turbo Expo 2005: Power for Land, Sea, and Air June 6-9, 2005, Reno-Tahoe, Nevada, USA.

[10]J. R. Kalb and T. Sattelmayer, "Lean Blowout Limit and NOx-Production of a Premixed Sub-PPM NOx Burner with Periodic Flue Gas Recirculation," GT 2004-53410, Proceedings of ASME Turbo Expo 2004.

[11]Turns, S. R., "An Introduction to Combustion: Concepts and Applications," 2nd edition, McGraw-Hill, pp. 331-342, 2000.